ISSN 1070-3284, Russian Journal of Coordination Chemistry, 2014, Vol. 40, No. 10, pp. 748–756. © Pleiades Publishing, Ltd., 2014.
Original Russian Text © E.V. Korneeva, T.A. Rodina, A.V. Ivanov, A.V. Gerasimenko, A.-C. Larsson, 2014, published in Koordinatsionnaya Khimiya, 2014, Vol. 40, No. 10, pp. 631–640.

Polymeric Gold(I) Diisobutyl Dithiophosphate, $[Au_2\{S_2P(O\text{-}iso\text{-}C_4H_9)_2\}_2]_n$: Synthesis, Supramolecular Self-Organization (a Role of Aurophilic Interaction), ^{13}C and ^{31}P MAS NMR Spectroscopy, and Thermal Behavior

E. V. Korneeva[a], T. A. Rodina[b], A. V. Ivanov[a, *], A. V. Gerasimenko[c], and A.-C. Larsson[d]

[a] *Institute of Geology and Nature Management, Far East Branch, Russian Academy of Sciences, Blagoveshchensk, 675000 Russia*

[b] *Amur State University, Blagoveshchensk, 675027 Russia*

[c] *Institute of Chemistry, Far East Branch, Russian Academy of Sciences, pr. Stoletiya Vladivostoka 159, Vladivostok, 690022 Russia*

[d] *Luleä University of Technology, S-97187, Luleä, Sweden*

**e-mail: alexander.v.ivanov@chemist.com*

Received February 15, 2014

Abstract—A new polymeric gold(I) diisobutyl dithiophosphate (Dtph), $[Au_2\{S_2P(O\text{-}iso\text{-}C_4H_9)_2\}_2]_n$ (**I**), was preparatively obtained and characterized by ^{13}C and ^{31}P MAS NMR spectroscopy and X-ray diffraction (CIF file CCDC no. 977818). Diagrams of the χ^2 statistic were constructed from the complete ^{31}P MAS NMR spectra and used to calculate the ^{31}P chemical shift anisotropy ($\delta_{aniso} = \delta_{zz} - \delta_{iso}$) and the asymmetry parameter $\eta = (\delta_{yy} - \delta_{xx})/(\delta_{zz} - \delta_{iso})$. The main structural unit of complex **I** is the noncentrosymmetric dinuclear molecule $[Au_2\{S_2P(O\text{-}iso\text{-}C_4H_9)_2\}_2]$, in which the gold atoms are linked by two bridging ligands Dtph. The central cyclic structural fragment of the dimer $[Au_2S_4P_2]$ is additionally stabilized by the intramolecular aurophilic interaction Au···Au. Further supramolecular self-organization of the complex involves intermolecular aurophilic bonds Au···Au that serve to unite adjacent dinuclear molecules $[Au_2\{S_2P(O\text{-}iso\text{-}C_4H_9)_2\}_2]$ with different spatial orientations into the polymer chains $([Au_2\{S_2P(O\text{-}iso\text{-}C_4H_9)_2\}_2])_n$. The thermal behavior of complex **I** was examined by synchronous thermal analysis under argon. The character of the thermolysis of the complex to reduced metallic gold as a final product was determined.

DOI: 10.1134/S1070328414100042

Gold(I) O,O'-dialkyl dithiophosphates [1–4] are of interest because of an unusual type of their polymeric structures formed predominantly by the intermolecular aurophilic interaction Au···Au [5–8]. The latter makes these complexes luminescent and allows them to be used as sensors of volatile chemical agents [2]. Earlier, using X-ray diffraction and ^{13}C and ^{31}P MAS NMR spectroscopy, we have studied polymeric gold(I) dialkyl dithiophosphates of the general formula $[Au_2\{S_2P(OR)_2\}_2]_n$ (R = *iso*-C_3H_7 [3] or *cyclo*-C_6H_{11} [4]). The latter complex features an atypical way of forming a polymeric structure, involving pairs of intermolecular secondary Au···S bonds (rather than aurophilic Au···Au interactions as it usually is).

Since the literature data on dialkyl dithiophosphate complexes are scarce [1–4] (in contrast to gold(I) dialkyl dithiophosphonates [9–13] and gold(I) dialkyl dithiophosphinates [14–17]), here we preparatively obtained a new polymeric gold(I) diisobutyl dithiophosphate of the formula $[Au_2\{S_2P(O\text{-}iso\text{-}C_4H_9)_2\}_2]_n$ (**I**) and determined its structure by ^{13}C and ^{31}P MAS NMR spectroscopy and X-ray diffraction. The thermal behavior of this complex was studied by synchronous thermal analysis (STA).

EXPERIMENTAL

For the synthesis of polymeric *catena*-poly[bis(μ_2-O,O'-diisobutyl dithiophosphato-S,S')digold(I)] (Au–Au) (**I**), potassium O,O'-diisobutyl dithiophosphate (**II**) (CHEMINOVA AGRO A/S, Denmark) was employed. All the solutions were used cooled to 0°C.

Synthesis of complex I. A solution of Na_2SO_3 (0.050 g) in distilled water (5 mL) was added to a solution of $Na[AuCl_4]$ (0.130 g). The resulting mixture was stirred to complete decoloration [18]. After completion of the reduction Au(III) $\longrightarrow$ Au(I), a solution of complex **II** (0.131 g, a 30% excess) was added. The reaction mixture was stirred and left in the cold for 2 h for maturation of a precipitate. The light yellow precipitate that formed was filtered off, washed with water, and dried on the filter. The yield of complex **I**

was 79%. The formation of gold(I) diisobutyl dithiophosphate can be written as follows:

$$2Na[AuCl_4] + 2Na_2SO_3 + 2K\{S_2P(O\text{-}iso\text{-}C_4H_9)_2\} + 2H_2O = [Au_2\{S_2P(O\text{-}iso\text{-}C_4H_9)_2\}_2] + 2KCl + 6NaCl + 2H_2SO_4.$$

Crystalline complexes **I** and **II** were characterized by ^{13}C MAS NMR spectroscopy:

I: (1 : 1 : 2) 76.6, 76.2 (1 : 1, $-OCH_2-$); 29.8, 29.6 (1 : 1, $-CH=$); 20.9, 20.7, 20.1, 19.8 (1 : 1 : 1 : 1, $-CH_3$).

II: (1 : 1 : 2) 75.1, 74.2, 73.5, 73.2, 72.9 ($-OCH_2-$); 29.9, 29.8, 29.7 ($-CH=$); 21.1, 21.0, 20.9, 20.8, 20.7, 20.6, 20.4, 20.3, 20.2, 20.1 ($-CH_3$).

Single crystals of complex **I** suitable for X-ray diffraction were grown from methanol.

$^{13}C/^{31}P$ CP/MAS NMR spectra were recorded on a CMX-360 spectrometer (Agilent/Varian/Chemagnetics InfinityPlus) operating at 90.52/145.73 MHz (superconducting magnet with B_0 = 8.46 T; Fourier transform). The $^1H-^{13}C$ and $^1H-^{31}P$ cross polarization techniques were used; $^{13}C-^1H$ and $^{31}P-^1H$ dipolar interactions were suppressed via proton decoupling in a magnetic field with the corresponding proton resonance frequency [19]. A sample (~60 mg) of complex **I** was packed into a ceramic (ZrO_2) rotor (4.0 mm in diameter). The spinning rates in $^{13}C/^{31}P$ MAS NMR experiments were 5500–6200(1)/2200–7600(1) Hz. The numbers of scans were 580–880/4, respectively. The proton $\pi/2$-pulse durations were 5.0/4.6 μs. The $^1H-^{13}C/^1H-^{31}P$ contact times were 2.5/2.5 ms; the pulses were spaced apart at 3.0/3.0 s. Isotropic ^{13}C and ^{31}P chemical shifts δ (ppm) are referenced to a line of crystalline adamantane used as an external standard (δ 38.48 ppm relative to tetramethylsilane) and 85% H_3PO_4. The width of the reference line of adamantane (2.6 Hz) was used to check the homogeneity of the magnetic field. The δ_{iso} values were corrected for drift of the magnetic field strength (its frequency equivalents for the $^{13}C/^{31}P$ nuclei were 0.051/0.11 Hz/h). The ^{31}P chemical shift anisotropy ($\delta_{aniso} = \delta_{zz} - \delta_{iso}$) and the asymmetry parameter ($\eta = (\delta_{yy} - \delta_{xx})/(\delta_{zz} - \delta_{iso})$) were calculated from diagrams of the χ^2 statistic [20]. The diagrams were plotted by analyzing the integral intensity ratios of the sidebands (due to spinning) [21, 22] in the complete ^{31}P MAS NMR spectra recorded at different spinning rates. The calculations were performed with the Mathematica program [23].

X-ray diffraction study of complex **I** was performed at 200(2) K on a BRUKER Kappa APEX2 CCD diffractometer (MoK_α radiation, graphite monochromator) for a twin crystal. The crystal–detector distance was 60 mm. The domains are mutually oriented at an angle of ~180° in the direction of the reciprocal space vector [1 0 0]*. The numbers of reflections collected from the first and second domains were 47973 (7224 unique reflections) and 47504 (7140 unique reflections). The number of overlapping reflections from the two domains was 33084 (6994 unique reflections). All the reflections were combined and processed in an HKLF 5 file used for structure refinement. In the final cycle of refinement, the experimental data from the first domain were employed. The BASF parameter refined with the SHELXTL/PC program is 0.5135(8). Structure **I** was solved by the direct method and refined anisotropically (for non-hydrogen atoms) by the least-squares method on F^2. The hydrogen atoms were located geometrically and refined using a riding model. Experimental data were collected and edited, and the unit cell parameters were refined, with the APEX2 [24] and SAINT programs [25]. All calculations for structure determination and refinement were performed with the SHELXTL/PC programs [26].

Selected crystallographic parameters and a summary of data collection and refinement for structure **I** are given in Table 1. Bond lengths and bond angles in structure **I** are listed in Table 2. Atomic coordinates, bond lengths, and bond angles for structure **I** have been deposited with the Cambridge Crystallographic Data Collection (no. 977818; deposit@ccdc.cam.ac.uk or http://www.ccdc.cam.ac.uk).

The thermal behavior of complex I was studied using the STA method by simultaneously recording TG and DSC curves. This study was carried out on a STA 449C Jupiter instrument (NETZSCH) in corundum crucibles. An opening in the cap of each crucible provided a vapor pressure of 1 atm during thermolysis. A sample (1.310–4.311 mg) was heated under argon to 1100°C at a heating rate of 5°C/min. To make the thermal effects in the low-temperature range more pronounced, measurements were performed in aluminum crucibles as well. The error in temperature measurements was ±0.7°C; the error in weight measurements was $\pm 1 \times 10^{-4}$ mg. TG and DSC curves were recorded using a correction file and temperature and sensitivity calibration data for a given temperature program and a given heating rate. The melting temperature of complex **I** was independently determined on a PTP(M) instrument (OAO Khimlaborpribor).

RESULTS AND DISCUSSION

The ^{13}C MAS NMR spectrum of complex **I** (Fig. 1) shows signals for the $-OCH_2-$, $-CH=$, and $-CH_3$ groups of the alkoxy substituents in the Dtph ligands. The presence of a single signal in the centroid of the complete ^{31}P MAS NMR spectrum suggests that the ^{31}P chemical shift tensor corresponds to an axial symmetry (Fig. 2, Table 3). The ^{31}P chemical shift of this signal (δ_{iso} = 103.4 ppm) is substantially lower than that for the starting potassium salt (Table 3). This lower value is due to covalent bonding between the Dtph groups and gold. For quantitative estimation of the ^{31}P chemical shift anisotropy and determination of structural functions of the dithiophosphate groups, we constructed diagrams of the χ^2 statistic (Fig. 3) as a

Table 1. Crystallographic parameters and the data collection and refinement statistics for structure **I**

Parameter	Value
Empirical formula	$C_{16}H_{36}O_4P_2S_4Au_2$
M	876.56
Crystal system	Monoclinic
Space group	$P2_1/c$
a, Å	9.3114(2)
b, Å	24.6745(4)
c, Å	12.0263(2)
β, deg	92.5455(8)
V, Å^3	2760.37(9)
Z	4
ρ_{calcd}, g/cm^3	2.109
μ, mm^{-1}	11.054
F(000)	1664
Crystal shape (dimensions, mm)	Prism (0.43 × 0.30 × 0.11)
θ scan range, deg	1.89–34.98
Ranges of h, k, and l indices	$-14 \le h \le 14$, $0 \le k \le 39$, $0 \le l \le 19$
Number of measured reflections	128561
Number of unique reflections	11882
Number of reflections with $I > 2\sigma(I)$	9183
Number of parameters refined	262
GOOF	1.098
R factors for $F^2 > 2\sigma(F^2)$	$R_1 = 0.0429$, $wR_2 = 0.1072$
R factors for all reflections	$R_1 = 0.0662$, $wR_2 = 0.1198$
Residual electron density (min/max), eÅ^{-3}	−3.022/4.340

function of δ_{aniso} and η. At $\eta = 0$, the ^{31}P chemical shift tensor is axially symmetric. An increase in η from 0 to 1 reflects an increasing contribution of the rhombic component. For complex **I**, η is 0.06; this value is indicative of a predominantly axial symmetry of the ^{31}P chemical shift tensor. The direction of the ^{31}P MAS NMR spectra corresponds to δ_{zz} (47.5 ± 0.3 ppm) < δ_{yy} (129.8 ± 1.6 ppm) ≈ δ_{xx} (133.0 ± 1.6 ppm), thus accounting for the negative sign of δ_{aniso} (−55.9 ppm).

Previous studies of di-, tetra-, hexa-, and polynuclear dithiophosphates of zinc [27, 28], cadmium [29, 30], lead(II) [31, 32], silver(I) [33], thallium(I) [34, 35], and gold(I) [3, 4] have demonstrated that the negative δ_{aniso} value is a characteristic feature of bridging Dtph ligands. The absolute value of δ_{aniso} usually correlates with the SPS angle: the greater the SPS angle, the higher $|\delta_{aniso}|$ [27]. The experimental $|\delta_{aniso}|$ value = 55.9 ppm suggests that the SPS angle for the bridging ligands in structure **I** is expected to be greater than 116.42° (found for $[Au_2\{S_2P(O\text{-}cyclo\text{-}C_6H_{11})_2\}_2]_n$ at $|\delta_{aniso}| = 44.6$ ppm [4]) and greater than 117.16°–117.39° (for $[Au\{S_2P(O\text{-}iso\text{-}C_3H_7)_2\}_2]_n$ [3] at $|\delta_{aniso}| = 47.9$–54.7 ppm) (Table 3).

To verify the conclusions drawn from ^{31}P MAS NMR data, we determined the crystal structure of complex **I** by X-ray diffraction.

The unit cell of complex **I** consists of four structurally equivalent noncentrosymmetric dinuclear molecules $[Au_2\{S_2P(O\text{-}iso\text{-}C_4H_9)_2\}_2]$ (Fig. 4). In these molecules, both nonequivalent dithiophosphate ligands bridge two gold atoms to form the extended eight-membered chelate ring $[Au_2S_4P_2]$ (Fig. 5).

As expected from the ^{31}P MAS NMR data, the SPS angles in both Dtph ligands (118.20° and 118.88°) appreciably exceed 117.39°. Nevertheless, it should be noted that the X-ray diffraction and ^{31}P MAS NMR data are formally inconsistent because the latter method cannot distinguish between nonequivalent Dtph ligands. This can be explained as follows: the isotropic ^{31}P chemical shift of dithiophosphate groups is affected most substantially by the structural function as well as by the strength of their coordination to metal; however, only one of four Au–S bonds in structure **I** reliably (though only slightly) differs in length from the others (Table 2).

The Au–S bond lengths vary in a narrow range (2.2913–2.3025 Å). The somewhat less strongly coordinated Dtph ligand containing the P(2) atom forms the S–Au(1,2) bonds of equal length (2.3025 Å), while the S–Au(1,2) bonds formed by the second, P(1)-containing ligand reliably differ in strength (2.3004 and 2.2913 Å). The dinuclear molecule $[Au_2\{S_2P(O\text{-}iso\text{-}C_4H_9)_2\}_2]$ is additionally stabilized by an intramolecular aurophilic interaction between the gold atoms: the Au(1)–Au(2) distance (2.9875 Å) is substantially shorter than the double van der Waals radius of the gold atom (3.32 Å) [36–38]. That is why the dinuclear molecule is distorted by contraction

Table 2. Selected bond lengths *d*, bond angles ω, and torsion angles φ in structure **I***

Bond	*d*, Å	Bond	*d*, Å
Au(1)–Au(2)	2.9875(3)	P(1)–O(2)	1.566(4)
Au(1)–Au(2)[a]	3.0553(3)	P(2)–O(3)	1.566(4)
Au(1)–S(1)	2.3004(15)	P(2)–O(4)	1.578(4)
Au(2)–S(2)	2.2913(17)	O(1)–C(1)	1.460(7)
Au(1)–S(3)	2.3025(14)	O(2)–C(5)	1.470(7)
Au(2)–S(4)	2.3025(16)	O(3)–C(9)	1.468(8)
P(1)–S(1)	2.011(2)	O(4)–C(13)	1.474(7)
P(1)–S(2)	2.013(2)	C(1)–C(2)	1.511(9)
P(2)–S(3)	2.014(2)	C(5)–C(6)	1.497(10)
P(2)–S(4)	2.004(2)	C(9)–C(10)	1.510(10)
P(1)–O(1)	1.568(4)	C(13)–C(14)	1.493(8)
Angle	ω, deg	Angle	ω, deg
Au(1)Au(2)Au(1)[b]	170.561(11)	S(4)Au(2)Au(1)	97.03(4)
Au(2)Au(1)Au(2)[a]	169.492(11)	S(4)Au(2)Au(1)[b]	85.29(4)
Au(1)S(1)P(1)	102.04(7)	S(1)P(1)S(2)	118.88(10)
Au(1)S(3)P(2)	98.07(7)	S(1)P(1)O(1)	112.2(2)
Au(2)S(2)P(1)	110.43(8)	S(1)P(1)O(2)	107.8(2)
Au(2)S(4)P(2)	102.59(7)	S(2)P(1)O(1)	109.9(2)
S(1)Au(1)Au(2)	92.06(4)	S(2)P(1)O(2)	108.3(2)
S(1)Au(1)Au(2)[a]	94.31(4)	O(1)P(1)O(2)	97.5(2)
S(1)Au(1)S(3)	176.73(6)	S(3)P(2)S(4)	118.20(10)
S(2)Au(2)Au(1)	92.02(4)	S(3)P(2)O(3)	112.7(2)
S(2)Au(2)Au(1)[b]	86.30(4)	S(3)P(2)O(4)	107.0(2)
S(2)Au(2)S(4)	170.35(5)	S(4)P(2)O(3)	106.7(2)
S(3)Au(1)Au(2)	89.10(3)	S(4)P(2)O(4)	108.1(2)
S(3)Au(1)Au(2)[a]	85.00(3)	O(3)P(2)O(4)	103.1(3)
Angle	φ, deg	Angle	φ, deg
S(1)Au(1)Au(2)S(2)	–36.65(6)	S(3)Au(1)Au(2)S(4)	–30.24(6)
S(1)Au(1)Au(2)S(4)	146.70(6)	S(3)Au(1)Au(2)S(2)	146.41(6)
Au(1)S(1)P(1)S(2)	–46.04(12)	Au(2)S(4)P(2)S(3)	39.64(12)
Au(2)S(2)P(1)S(1)	14.43(14)	Au(1)S(3)P(2)S(4)	–66.66(10)

* The symmetry operation codes are [a] $x, -y + 1/2, z + 1/2$; [b] $x, -y + 1/2, z - 1/2$.

Table 3. Parameters of the ^{31}P MAS NMR spectra of crystalline gold(I) dialkyl dithiophosphates

Complex	^{31}P		
	δ_{iso}, ppm	$^{*}\delta_{aniso}$, ppm	$^{*}\eta$
$[Au_2\{S_2P(O\text{-}iso\text{-}C_4H_9)_2\}_2]_n$ (I)	103.4 ± 0.2	−55.9 ± 0.2	0.06 ± 0.06
$[Au_2\{S_2P(O\text{-}iso\text{-}C_3H_7)_2\}_2]_n$ [3] (1 : 1 : 1 : 1)	103.0 (25)**	−56.4 ± 1.0	0.54 ± 0.07
	102.0 (24)**	−54.7 ± 1.0	0.50 ± 0.08
	97.3 (26)**	−50.6 ± 0.8	0.43 ± 0.10
	96.2 (24)**	−47.9 ± 1.0	0.30 ± 0.17
$[Au_2\{S_2P(O\text{-}cyclo\text{-}C_6H_{11})_2\}_2]_n$ [4]	94.8	−44.6 ± 0.4	0.82 ± 0.02
$K\{S_2P(O\text{-}iso\text{-}C_4H_9)_2\}$ [27]	110.9	−123.0 ± 2.0	0.01 ± 0.14

* $\delta_{aniso} = \delta_{zz} - \delta_{iso}$; $\eta = (\delta_{yy} - \delta_{xx})/(\delta_{zz} - \delta_{iso})$.

** The ^{31}P–^{31}P coupling constants ^4J in herzes.

along the Au(1)–Au(2) line; for comparison, the distances between the sulfur atoms within the ligand are 3.466 and 3.448 Å (the van der Waals radius of the S atom is 1.80 Å [36–38]). This interaction also results in deviation of the angles S(1)Au(1)S(3) and S(2)Au(2)S(4) from 180°: 176.73° and 170.35°, respectively.

The geometry of the central chelate ring $[Au_2S_4P_2]$ in dinuclear complex **I** corresponds to none of ten stable canonical conformations calculated for eight-membered rings [39]. For this reason, the cyclic framework of this molecule should be regarded as five-membered rings $[Au_2S_2P]$ fused along the Au–Au bond. The torsion angles S(1)Au(1)Au(2)S(2) (−36.65(6)°) and S(3)Au(1)Au(2)S(4) (−30.24(6)°) suggest that the Au and S atoms are substantially not coplanar (the coplanar arrangement of the atoms under consideration is characteristic of the envelope conformation). In turn, the torsion angles S(1)Au(1)Au(2)S(4) (146.70(6)°) and S(3)Au(1)Au(2)S(4) (146.41(6)°) characterize the mutual orientation of these five-membered rings, and the opposite signs of the angles Au(1)S(1)P(1)S(2) (−46.04(12)°) and Au(2)S(4)P(2)S(3) (39.64(12)°) (Table 2) indicate their opposition in direction. Clearly, the five-membered rings $[Au_2S_2P]$ in structure **I** adopt two *twist*-configurations with opposite orientations.

Subsequent supramolecular self-organization of complex **I** involves an intermolecular aurophilic interaction (Au(1)···Au(2)[a] 3.0553(3) Å), which is somewhat weaker than the intramolecular one. As a result, each dinuclear molecule $[Au_2\{S_2P(O\text{-}iso\text{-}C_4H_9)_2\}_2]$ are bound by aurophilic interactions to its two nearest neighbors[1], which gives rise to a zigzag polymer chain: the Au(1)Au(2)Au(1)[b] angle is 170.561(11)° and the Au(2)Au(1)Au(2)[a] angle is 169.492(11)°. The different spatial orientations of dinuclear molecules that

[1] Interestingly, dinuclear gold(I) diisobutyl dithiophosphinate, which is similar in both composition and structure, shows no intermolecular aurophilic bonds [16].

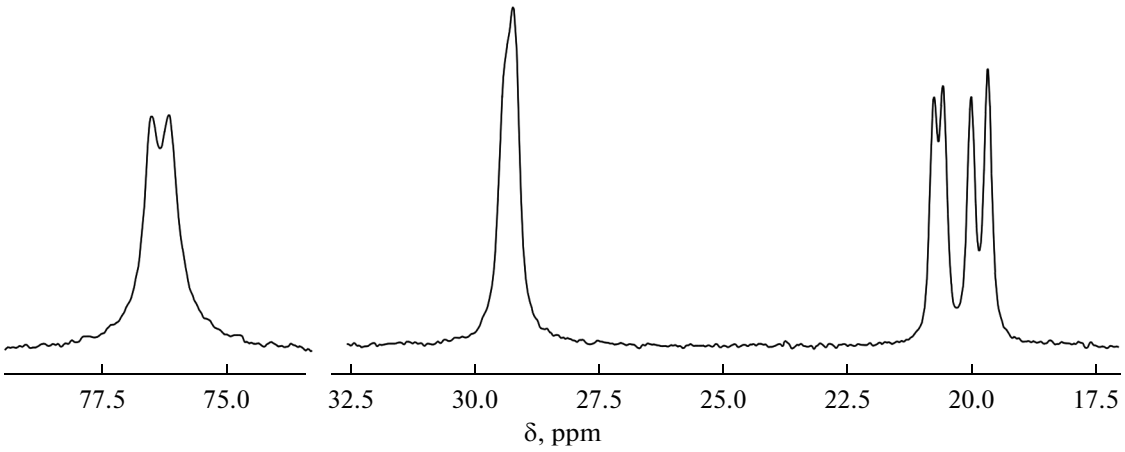

Fig. 1. ^{13}C MAS NMR spectrum of complex **I**. The number of scans/spinning rate is 880/6.2 kHz.

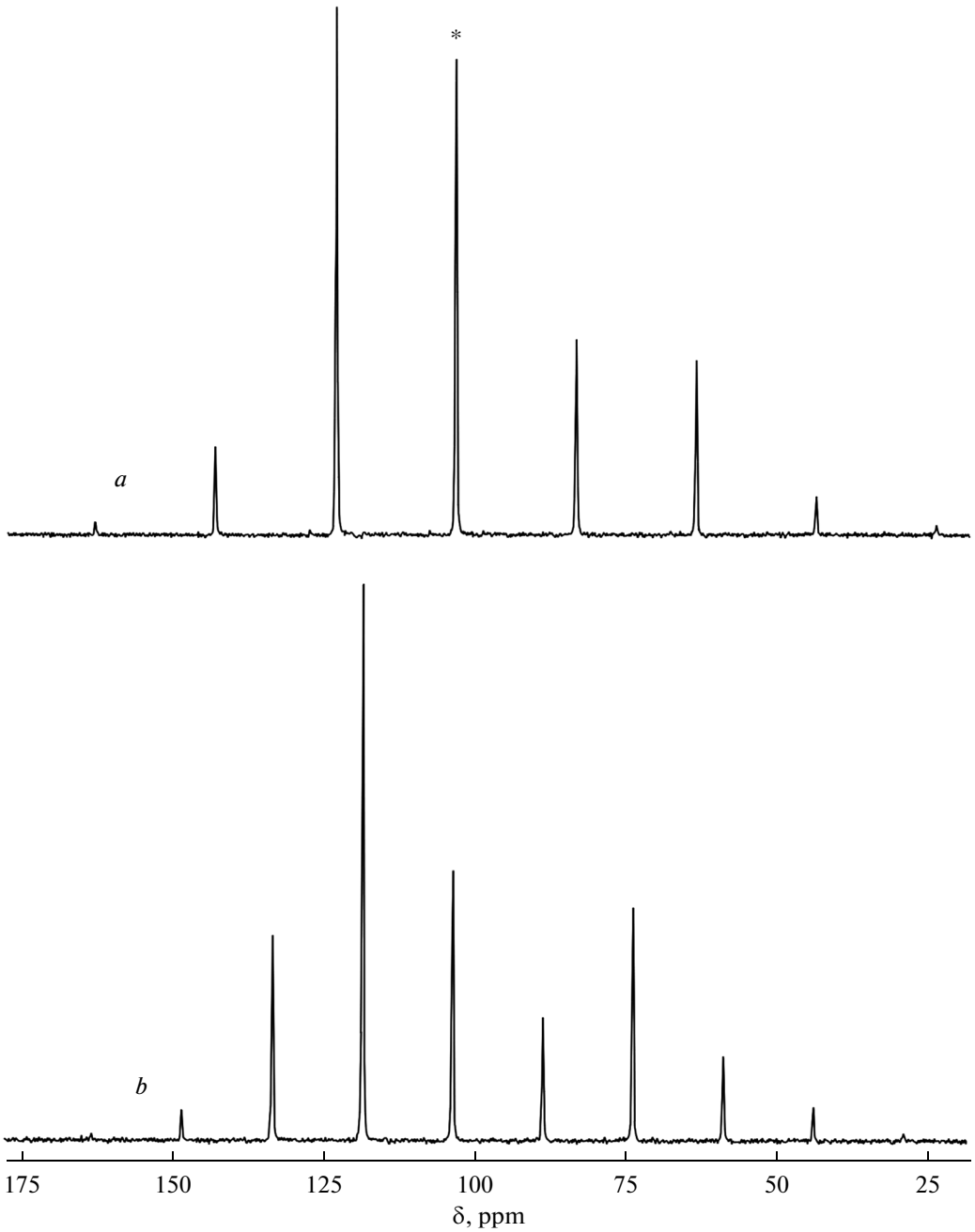

Fig. 2. ^{31}P MAS NMR spectra of complex **I** at two spinning rates: (*a*) 2.9 and (*b*) 2.2 kHz.

alternate along the polymer chain are due to an angle of ~90° between them (Fig. 4).

In the polymer chain under discussion, both gold atoms are in the distorted rhombic environment $[S_2Au_2]$, which suggests the outer-orbital sp^2d-hybrid state of the complexing agent. The longer axis of the rhombs is given by the gold atoms Au–Au–Au (6.042 Å) and the shorter axes, by S–Au–S (4.603 and 4.594 Å). Because complex **I** contains direct Au–Au bonds (both within and between dinuclear molecules), it can be classified as a cluster compound. The phosphorus atoms of the Dtph ligands are in the distorted tetrahedral environment $[O_2S_2]$. The P–S bond length (2.004–2.014 Å) is intermediate between idealized single (2.14 Å) and double (1.94 Å) phosphorus–sulfur bonds [40], which is due to electron density delocalization over the structural fragments PS_2.

The thermal behavior of polymeric gold(I) diisobutyl dithiophosphate was studied by STA (simultaneous recording of TG and DSC curves) under argon. The TG curve shows three steps of weight loss (Fig. 6*a*). The first step (160–250°C) due to the ther-

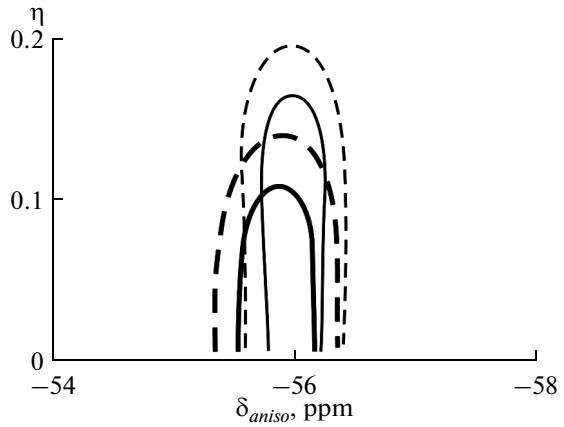

Fig. 3. Diagrams of the χ^2 statistic (as a function of the parameters of the ^{31}P chemical shift anisotropy) for the signal in the ^{31}P NMR spectra of $[Au_2\{S_2P(O\text{-}iso\text{-}C_4H_9)_2\}_2]_n$ at spinning rates of 2.2 and 2.9 kHz (thick and thin lines, respectively). The solid and dashed lines bound the 68.3 and 95.4% confidence regions, respectively, for δ_{aniso} and η.

molysis proper of complex **I** reflects the greatest weight loss (35.80%). Differentiation of the TG curve revealed that the weight loss rate is maximum at 198.8°C. The two other, flattened and indistinct steps at 250–520°C (8.51%) and 520–960°C (4.76%) are due to the desorption of the thermolysis products. The weight of the residue (50.78%) at 1100°C exceeds that calculated for metallic gold (44.94%) by 5.84%. When the crucible was opened upon completion of the process, numerous small gold beads were observed on its bottom surface. The interior surface of the crucible and its cap also showed a dark gray deposit of carbon formed in an inert atmosphere; the presence of this carbon accounts for the discrepancy between the calculated and experimental weights of the residue.

The DSC curve shows several thermal effects (Figs. 6*b*, 6*c*). The endothermic effect in the low-temperature range (before any weight loss) is due to melting of the sample (extrapolated T_m = 70.6°C). In an independent way, we determined that complex **I** melts at 70°C. The use of an aluminum crucible for DSC measurements allowed us to resolve the thermal effect

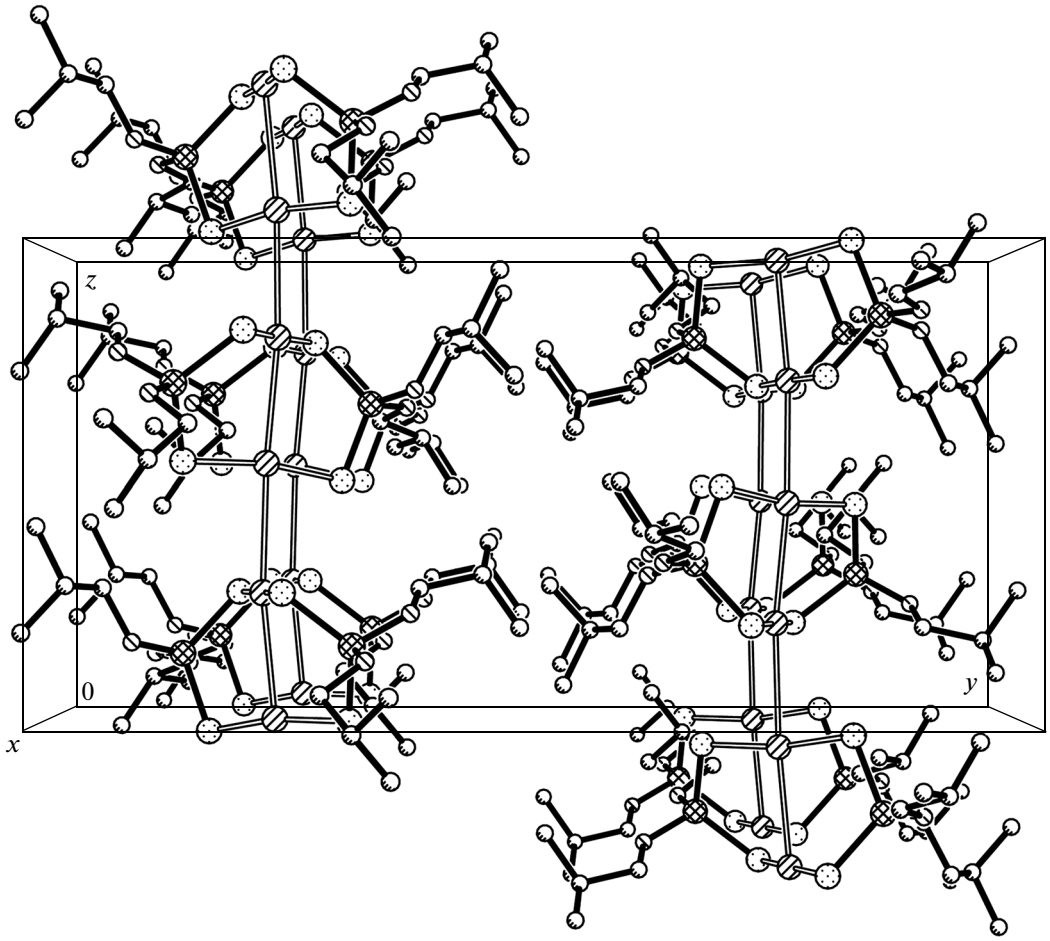

Fig. 4. Crystal packing of complex **I**.

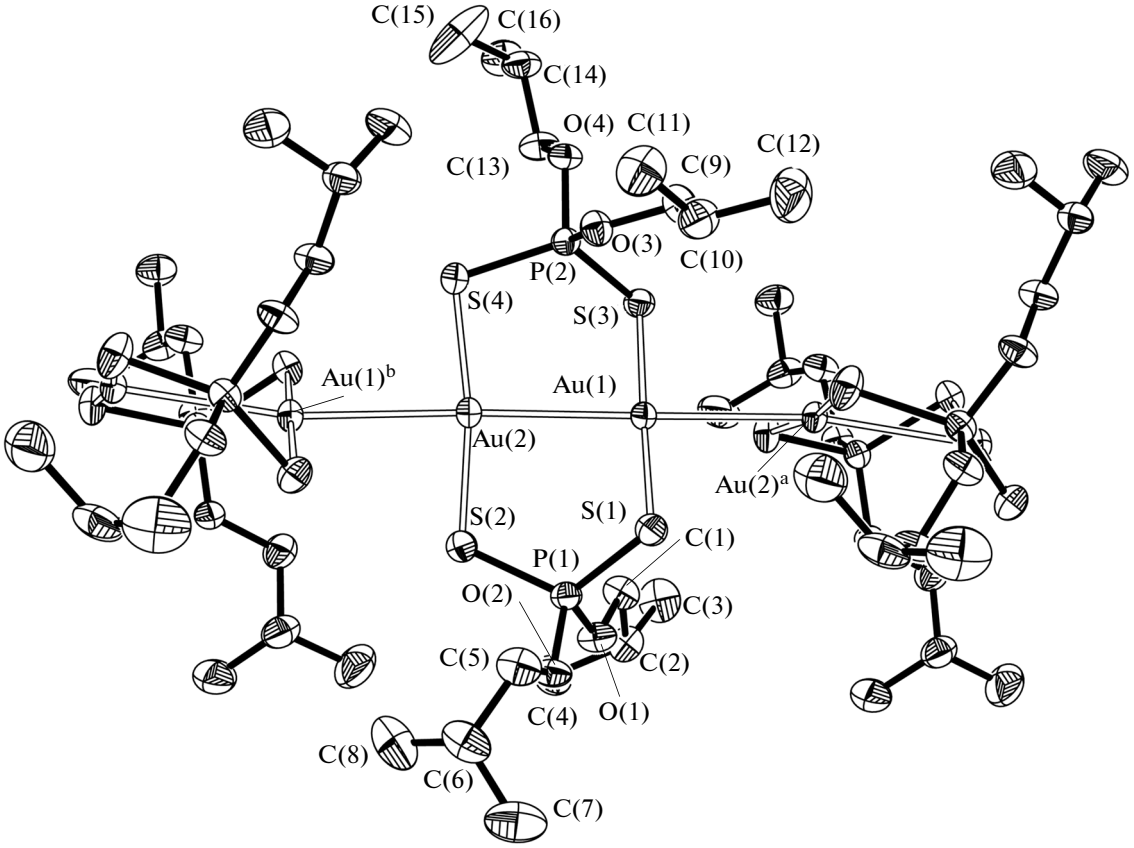

Fig. 5. Three-unit structural fragment of the polymer chain of complex **I** with atomic displacement ellipsoids (50% probability).

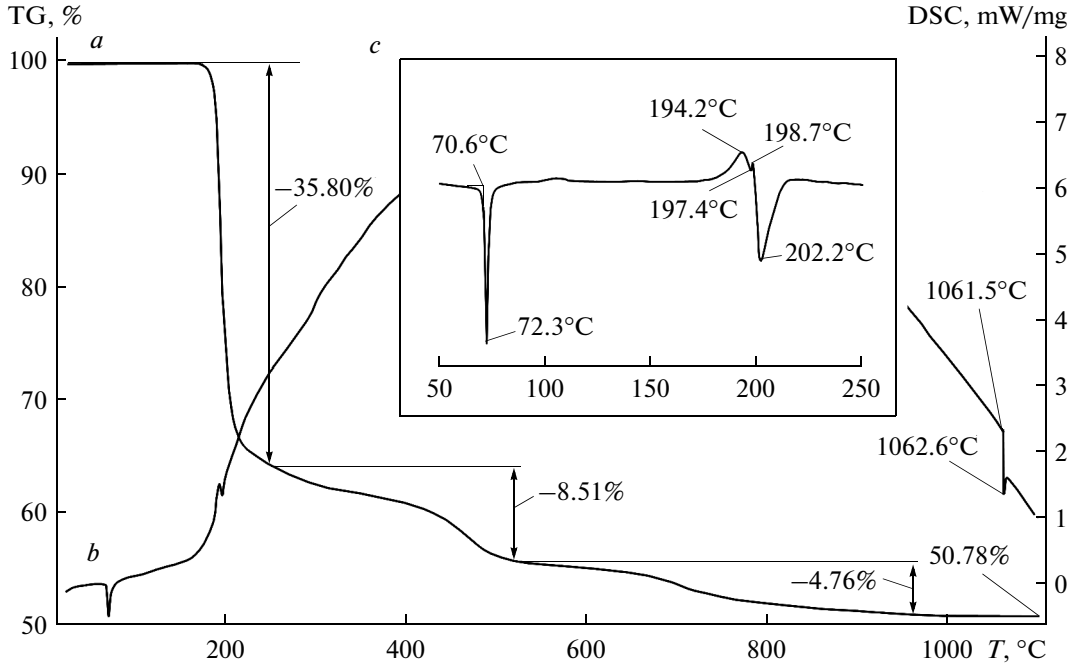

Fig. 6. (*a*) TG and (*b, c*) DSC curves of complex **I**. (*c*) The low-temperature range of the DSC curve for a sample in an aluminum crucible.

in the first (main) step of weight loss. It can be seen in Fig. 6*c* that this effect is a superposition of exothermic (at 194.2°C) and endothermic effects (at 202.2°C), which reflects a complicated character of the thermolysis of the complex. The high-temperature endothermic effect is due to the melting of reduced gold (extrapolated T_m= 1061.5°C).

ACKNOWLEDGMENTS

We are grateful to CHEMINOVA AGRO A/S (Denmark) for providing potassium O,O'-diisobutyl dithiophosphate.

This work was supported by the Presidium of the Russian Academy of Sciences (Basic Research Program "Development of Methods for the Synthesis of Chemical Compounds and for the Design of Novel Materials", project no. 12-I-P8-01) and the Presidium of the Far East Branch of the Russian Academy of Sciences (project no. 12-III-A-04-040).

REFERENCES

1. Lawton, S.L., Rohrbaugh, W.J., and Kokotailo, G.T., *Inorg. Chem.*, 1972, vol. 11, no. 9, p. 2227.
2. Lee, Y.-A., McGarrah, J.E., Lachicotte, R.J., and Eisenberg, R., *J. Am. Chem. Soc.*, 2002, vol. 124, no. 36, p. 10662.
3. Ivanov, A.V., Lutsenko, I.A., Korneeva, E.V., et al., *Rus. J. Coord. Chem.,* 2012, vol. 38, no. 6, p. 430.
4. Ivanov, A.V., Korneeva, E.V., Lutsenko, I.A., et al., *J. Mol. Struct.*, 2013, vol. 1034, p. 152.
5. Schmidbaur, H., *Gold Bull.*, 2000, vol. 33, no. 1, p. 3.
6. Uson, R., Laguna, A., Laguna, M., et al., *Chem. Commun.*, 1988, no. 11, p. 740.
7. Pathaneni, S.S. and Desiraju, G.R., *Dalton Trans.*, 1993, no. 2, p. 319.
8. Cao, L., Jennings, M.C., and Puddephatt, R.J., *Inorg. Chem.*, 2007, vol. 46, no. 4, p. 1361.
9. Staples, R.J. and Fackler, Jr., J.P., *Inorg. Chem. Commun.*, 1998, vol. 1, no. 2, p. 51.
10. Zyl van, W.E., Lopez-de-Luzuriaga, J.M., and Fackler, J.P., Jr., *J. Mol. Struct.*, 2000, vol. 516, no. 1, p. 99.
11. Zyl van, W.E., Lopez-de-Luzuriaga, J.M., and Mohamed, A.A., et al., *Inorg. Chem.*, 2002, vol. 41, no. 17, p. 4579.
12. Maspero, A., Kani, I., Mohamed, A.A., et al., *Inorg. Chem.*, 2003, vol. 42, no. 17, p. 5311.
13. Karakus, M., Lonnecke, P., Hildebrand, M., and Hey-Hawkins, E., *Z. Anorg. Allg. Chem.*, 2011, vol. 637, nos. 7–8, p. 983.
14. Siasios, G. and Tiekink, E.R.T., *Z. Kristallogr.*, 1995, vol. 210, p. 698.
15. Preisenberger, M., Bauer, A., Schier, A., and Schmidbaur, H., *Dalton Trans.*, 1997, no. 24, p. 4753.
16. Gysling, H.J., Blanton, T.N., McMillan, S.M., and Lushington, K.J., *Z. Kristallogr.*, 1999, vol. 214, p. 309.
17. Zyl van, W.E., Lopez-de-Luzuriaga, J.M., and Fackler, J.P., Jr., and Staples, R.J., *Can. J. Chem.*, 2001, vol. 79, nos. 5–6, p. 896.
18. Miller, J.B. and Burmeister, J.L., *Synth. React. Inorg. Met.-Org. Chem.,* 1985, vol. 15, no. 2, p. 223.
19. Pines, A., Gibby, M.G., and Waugh, J.S., *J. Chem. Phys.*, 1972, vol. 56, no. 4, p. 1776.
20. Press, W.H., Teukolsky, S.A., Vetterling, W.T., and Flannery, B.P., *Numerical Recipes*, Cambridge: Univ. Press, 1994.
21. Hodgkinson, P. and Emsley, L., *J. Chem. Phys.*, 1997, vol. 107, no. 13, p. 4808.
22. Antzutkin, O.N., Lee, Y.K., and Levitt, M.H., *J. Magn. Reson.*, 1998, vol. 135, no. 1, p. 144.
23. Wolfram, S., *The Mathematica Book*, Cambridge: Wolfram Media/Cambridge Univ., 1999, p. 1470.
24. *APEX2*, Madison (WI, USA): Bruker AXS, 2010.
25. *SAINT*, Madison (WI, USA): Bruker AXS, 2010.
26. Sheldrick, G.M., *Acta Crystallogr., Sect. A: Found. Crystallogr.*, 2008, vol. 64, no. 1, p. 112.
27. Larsson, A.-C., Ivanov, A.V., Forsling, W., et al., *J. Am. Chem. Soc.*, 2005, vol. 127, no. 7, p. 2218.
28. Ivanov, A.V., Antzutkin, O.N., Larsson, A.-C., et al., *Inorg. Chim. Acta*, 2001, vol. 315, no. 1, p. 26.
29. Ivanov, A.V., Loseva, O.V., Ivanov, M.A., et al., *Russ. J. Inorg. Chem.*, 2007, vol. 52, no. 10, p. 1595.
30. Ivanov, A.V., Gerasimenko, A.V., Antzutkin, O.N., and Forsling, W., *Inorg. Chim. Acta*, 2005, vol. 358, no. 9, p. 2585.
31. Larsson, A.-C., Ivanov, A.V., Antzutkin, O.N., et al., *Inorg. Chim. Acta*, 2004, vol. 357, no. 9, p. 2510.
32. Larsson, A.-C., Ivanov, A.V., Pike, K.J., et al., *J. Magn. Reson.*, 2005, vol. 177, no. 1, p. 56.
33. Ivanov, A.V., Zinkin, S.A., Gerasimenko, A.V., et al., *Rus. J. Coord. Chem.,* 2007, vol. 33, no. 1, p. 20.
34. Rodina, T.A., Ivanov, A.V., Konfederatov, V.A., et al., *Russ. J. Inorg. Chem.*, 2009, vol. 54, no. 11, p. 1779.
35. Ivanov, A.V., Konfederatov, V.A., Gerasimenko, A.V., Larsson, A.C., *Rus. J. Coord. Chem.,* 2009, vol. 35, no. 11, p. 857.
36. Pauling, L., *The Nature of the Chemical Bond and the Structure of Molecules and Crystals*, London: Cornell Univ., 1960.
37. Bondi, A., *J. Phys. Chem.*, 1964, vol. 68, no. 2, p. 441.
38. Bondi, A., *J. Phys. Chem.*, 1966, vol. 70, no. 9, p. 3006.
39. Evans, D.G. and Boeyens, J.C.A., *Acta Crystallogr., Sect. B: Struct. Sci.*, 1988, vol. 44, no. 6, p. 663.
40. Lawton, S.L. and Kokotailo, G.T., *Inorg. Chem.*, 1969, vol. 8, no. 11, p. 2410.

Translated by D. Tolkachev